Dual-Responsive Fe_3O_4@Polyaniline Chiral Superstructures for Information Encryption

*Zuyang Ye[1], Zhiwei Li[1], Ji Feng[1], Chaolumen Wu[1], Qingsong Fan[1], Chen Chen[1], Jinxing Chen[1,2], and Yadong Yin[1,]**

[1]Department of Chemistry, University of California, Riverside, California 92521, United States

[2]Institute of Functional Nano and Soft Materials (FUNSOM), Jiangsu Key Laboratory for Carbon-Based Functional Materials and Devices, Soochow University, Suzhou 215123, China

*Corresponding Author: Email address: yadong.yin@ucr.edu

KEYWORDS: self-assembly, chirality, nanostructures, stimuli-responsive, dynamic modulation, information encryption

ABSTRACT: Incorporating stimuli-responsive mechanisms into chiral assemblies of nanostructures offers numerous opportunities to create optical materials capable of dynamically modulating their chiroptical properties. In this study, we demonstrate the formation of chiral superstructures by assembling Fe_3O_4@polyaniline hybrid nanorods using a gradient magnetic field. The resulting superstructures exhibit a dual response to changes in both the magnetic field and solution pH, enabling dynamic regulation of the position, intensity, and sign of its circular dichroism peaks. Such responsiveness allows for convenient control

over the optical rotatory dispersion properties of the assemblies, which are further integrated into the design of a chiroptical switch that can display various colors and patterns when illuminated with light of different wavelengths and polarization states. Finally, an optical information encryption system is constructed through the controlled assembly of the hybrid nanorods to showcase the potential opportunities for practical applications brought by the resulting responsive chiral superstructures.

Chirality is ubiquitous in nature, ranging from small molecules and polymers to living systems and even galaxies. It has always been a topic of interest to chemists,[1-3] especially in recent years with the emergence of various chiral nanomaterials.[4-6] Nanoparticles with chiral structures can interact with light to selectively absorb left- or right-handed circularly polarized light (CPL), known as circular dichroism (CD). There are two main strategies to generate chiral nanostructures. One strategy is the surface functionalization of achiral nanoparticles with chiral molecules to induce the chiral growth of the nanoparticles.[7-9] For instance, González-Rubio *et al.* demonstrated the use of chiral cosurfactants to template the growth of gold nanorods with screw-like helical structures.[9] Another strategy is to assemble achiral nanoparticles into chiral superstructures.[10, 11] Compared to the top-down fabrication methods, the bottom-up self-assembly processes offer simplicity and flexibility in constructing chiral plasmonic metamaterials and metasurfaces.[12-14] A notable approach involves DNA-assisted self-assembly, which uses DNA linkages to assemble plasmonic molecules with reconfigurable chirality. However, it requires specific designs of DNA linkages and faces potential challenges for large-area assembly.[15, 16] An alternative approach is to form the Bouligand helical structure by stacking two or more layers of one-dimensional assembled structures at an oblique angle.[17,

[18] The advantage of the assembly process is its reversibility, which allows for dynamic tuning of the chiral architecture.

Magnetic field-guided self-assembly provides rapid, reversible, and remote modulation of magnetic nanoparticles into reconfigurable superstructures across large areas.[19, 20] It has been shown that magnetic fields can be configured to induce chirality in magnetic particle assemblies.[21] We have further demonstrated that a gradient magnetic field is intrinsically chiral, allowing the assembly of magnetic nanoparticles into chiral superstructures with reversible field-dependent tunability.[22] One significant advantage of the magnetic assembly approach is that many optically active but nonmagnetic materials can be magnetically assembled to enable chirality through attachment or coating processes.[23, 24]

In this work, we demonstrate that the integration of stimuli-responsive optical materials with magnetic nanostructures can produce reconfigurable optical switches with highly tunable and controllable chiroptical properties, such as CD and ORD (optical rotatory dispersion), thus offering opportunities in many applications in the fields of chiral sensing, optical display, information encryption, and anti-counterfeiting.[25, 26] Specifically, we have developed hybrid nanostructures comprising of a magnetic Fe_3O_4 nanorod core and a pH-responsive polyaniline (PANI) shell.[27, 28] The Fe_3O_4@PANI hybrid nanorods possess the ability to self-assemble into chiral superstructures when their colloidal dispersion is exposed to a gradient magnetic field. The handedness of the resulting superstructures can be dynamically controlled by tuning the direction of the magnetic field. Moreover, the chiroptical properties can be finely tuned by manipulating the pH of the dispersion, thanks to the pH-responsive nature of PANI. This pH response enables a wide modulation range of circular dichroism (CD) signals. Under both acidic and basic conditions, the chiral structures generated can rotate the polarization states of incident light in both solution and solid films. As a result, when observed through crossed polarizers, highly tunable transmitted colors are produced. This exceptional capability allows

for the design of a chiral optical switch capable of regulating multiple colors. Different patterns can be created by illuminating the system with light of various wavelengths. To further demonstrate the advantages of the highly tunable chiroptical properties, we have developed a reconfigurable information encryption system that can display diverse information under both unpolarized and polarized light, showcasing its versatility and potential applications.

RESULTS AND DISCUSSION

Synthesis and Assembly of Fe_3O_4@PANI Nanorods. The magnetic nanorods were prepared by synthesizing FeOOH nanorods through the hydrolysis of $FeCl_3$ and further reduced to magnetic nanorods after surface modification with polyacrylic acid (PAA).[29, 30] The coating of PANI was initiated by mixing Fe_3O_4 cores with aniline monomers and ammonium persulfate as the oxidizing agent.[31] The UV-Vis spectrum of the resulting solution (**Fig. 1a**) showed absorption peaks at 325 nm and 570 nm, corresponding to the electronic transition from benzenoid state to π^* state and benzenoid state to quinoid state of the emeraldine base form of PANI (PANI-EB), respectively.[32, 33] The TEM image (**Fig. 1b**) of a typical sample confirmed the uniform coating of PANI on Fe_3O_4, with an average thickness of 23 nm.

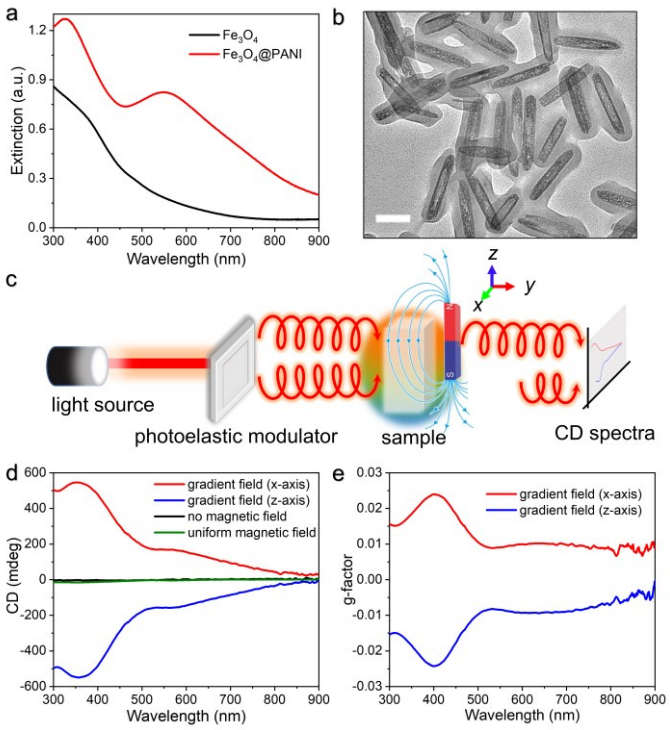

Figure 1. Magnetic assembly of chiral Fe_3O_4@PANI superstructures. (a) UV-Vis-NIR absorption spectra of Fe_3O_4 and Fe_3O_4@PANI nanorods. (b) TEM image of Fe_3O_4@PANI nanorods. Scale bar: 100 nm. (c) Schematic illustration of CD measurement of magnetic assembly of chiral superstructures. The blue arrows represent the magnetic field directions along the z-axis. (d) CD spectra and (e) anisotropic g-factor of the assembled chiral Fe_3O_4@PANI superstructures.

The as-synthesized Fe_3O_4@PANI nanorods were used as building blocks to create chiral superstructures under a gradient magnetic field generated by a single magnet positioned eccentrically toward the sample. The CD spectrometer was used to verify the chiroptical properties of the assembled structures (**Fig. 1c**). As shown in **Fig. 1d**, when the magnetic field was along the x-axis, the assembled structures exhibited distinct CD peaks at 358 nm and 570 nm, corresponding to the absorption wavelengths of PANI-EB. When we changed the magnetic field direction from the x to z-axis, the sample exhibited a symmetric CD spectrum, with the CD signal showing a comparable peak position and intensity but a reversed sign, indicating the

generation of chiral superstructures with opposite handedness. This result demonstrates the efficacy of magnetic assembly for creating and dynamic tuning the chirality of hybrid structures. The anisotropic g-factor values of the assembled structures were also calculated and shown in **Fig. 1e**. The maximum g-factor value approached 0.024, which was comparable to that of chiral PANI structures produced using other methods.[34, 35] In the absence of an external magnetic field, or with a uniform magnetic field produced by two facing identical magnets, no observable CD signals were detected (Fig, 1d).

pH-Responsive Chiroptical Properties. It is well understood that PANI-EB can be doped with protons to form the emeraldine salt state of PANI (PANI-ES). The doping process creates the radical cation structure, or the so-called polaron structure, as schematically illustrated in **Fig. 2a**. The formation of polarons leads to lattice distortion, resulting in two polaron electronic energy levels. Further increasing the doping level produces bipolaron energy states, reducing the energy required for electron transitions. When the pH of the Fe_3O_4@PANI aqueous dispersion was decreased, PANI was gradually transformed from PANI-EB to PANI-ES through proton doping. Accordingly, the color of the solution changed from magenta to cyan and green, which was consistent with the evolution of the UV-Vis-NIR absorption spectra shown in **Fig. 2b**. Two new absorption peaks appeared at around 400 nm and around 800 nm, which were assigned to polaron and bipolaron electronic transitions, respectively.

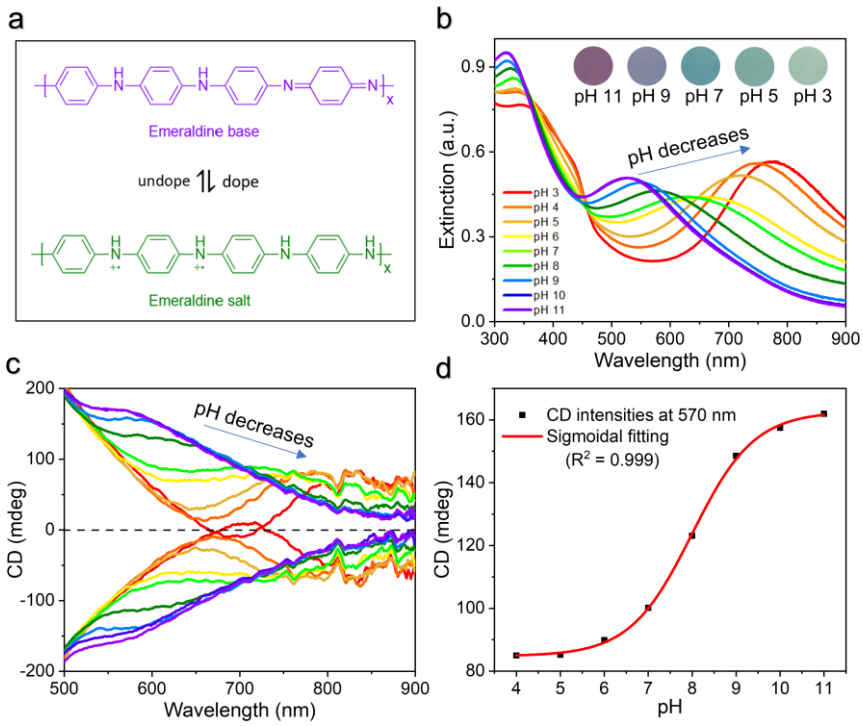

Figure 2. pH-responsive chiroptical properties of chiral Fe_3O_4@PANI superstructures. (a) Two different states of PANI. The emeraldine base is converted to emeraldine salt by doping with protons. The reaction is reversed by deprotonation. (b, c) The extinction spectra (b) and CD spectra (c) of the assembled chiral Fe_3O_4@PANI superstructures under different pH values. The insets in (b) show the color of the solution. Figures (b) and (c) share the same legend. (d) The changes of CD intensity at 570 nm in response to pH changes of the solution.

When the hybrid nanorods were assembled into chiral superstructures, the CD signal changed dramatically with decreasing pH, as shown in **Fig. 2c**. The peak originated from the benzenoid-to-quinoid transition of PANI-EB at 570 nm gradually weakened, while a new peak emerged at approximately 830 nm. Interestingly, when the pH value reached 3, a negative CD signal at around 700 nm appeared together with the signal around 830 nm, which was characteristic of the bisignate CD band from the bipolaron electronic transition. The bisignate band may be attributed to the chiral exciton coupling between adjacent polymer chains.[36] The CD and absorption peak positions shifted similarly at different pH values, indicating a good

correlation. Plotting the CD intensity changes against the pH values produces a sigmoidal curve (**Fig. 2d**). The peak intensity rose linearly when the pH increased from 6 to 9 but plateaued when the doping level was close to saturation or fully undoped. The above results confirm the dual responsiveness of the assembled superstructures, wherein the chiroptical properties can be manipulated not only by the external magnetic field but also by adjusting the pH values. Further, the dual-responsive chirality was shown to be fully reversible over repeated cycling between opposite magnetic field directions and pH values (Fig. S1). In addition, linear dichroism (LD) spectra of the superstructure dispersion verified a negligible contribution from linear polarization effects to the observed optical activity, as shown in Figure S2.

Optical Rotatory Dispersion. Chiral materials are optically active and can change the rotation of the plane of polarization of light as it passes through the material. The amount and direction of rotation depend on the wavelength of the incident light. This wavelength-dependent rotation is referred to as optical rotatory dispersion, ORD, which generates different transmission colors when light passes chiral materials and crossed polarizers. Figure S3 shows the schematic illustration of the experimental setup for measuring ORD. The unpolarized light first passes a linear polarizer, followed by the chiral material and the analyzer with the polarization direction perpendicular (denoted as 0°) to the first polarizer. Only the light with a significant degree of rotation can pass through the analyzer. Without the external magnetic field, no chirality was formed, and the solution with homogeneously dispersed nanorods could not induce any change in the plane of light polarization, leading to the dark color (Fig. S4). When the analyzer was rotated a small degree, we observed a faint color because a small fraction of incident light parallel to the analyzer could pass through.

When applying a gradient magnetic field, the chiral superstructures exhibited transmission colors under the ORD measurement setting, as exhibited in **Fig. 3a**. At 0°, the Fe_3O_4@PANI-EB displayed purple on the top and bottom layers under a magnetic field along

the x-axis (Fig. 3a(i)). Note that the middle region was black because the magnetic field in this region was relatively uniform, and therefore, no chiral superstructures were formed. Although the particles on the top and bottom layers showed similar purple colors, they were assembled into chiral structures with different handednesses. When the analyzer angle was rotated clockwise from 0° to 15°, they underwent different color changes, with the top layer turning brown and the bottom layer lavender (Fig. 3a(i)). On the other hand, when the analyzer angle was rotated counter-clockwise from 0° to -15°, the color changes of the top layer and the bottom layer were reversed. Symmetric color changes could also be observed when altering the magnetic field along the z-axis (Fig. 3a(ii)). Similarly, the assembled Fe_3O_4@PANI-ES chiral structures also showed color changes under ORD measurement, where the colors shifted from cyan to light green or dark brown, when rotating the analyzers from 0° to a higher angle (Fig. 3a(iii) and (iv)).

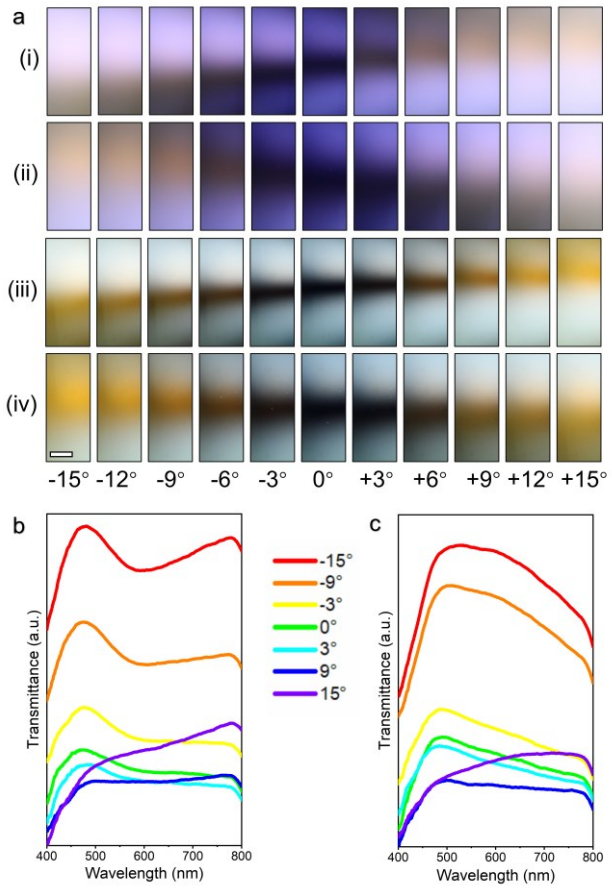

Figure 3. ORD measurement of chiral Fe_3O_4@PANI superstructures. (a) Polarization-resolved colors of light transmitted through chiral Fe_3O_4@PANI superstructures with (i) EB and (iii) ES under the x-axis of the magnetic field, and (ii) EB and (iv) ES under the z-axis of the magnetic field. The rotational angle of the analyzer was increased from −15° (left-most) to 15° (right-most). All the digital images share the same scale bar of 5 mm. (b, c) Transmittance spectra at different analyzer angles for EB (b) and ES (c) under a magnetic field along the x-axis.

To reveal the origin of the color changes of chiral superstructures under ORD measurements, the transmittance spectra were measured for the samples on the top layer with an external magnetic field along the x-axis (**Fig. 3b, c**). For Fe_3O_4@PANI-EB chiral structures at 0°, the spectra exhibited high transmission at 480 nm, leading to a purple color due to the

mixed transmitted light (**Fig. 3b**). The peak from 650 nm to 800 nm gradually increased as the analyzer angle was rotated towards higher values. The dip at around 600 nm was attributed to the characteristic absorption corresponding to the benzenoid-to-quinoid electronic transitions of PANI-EB, which resulted in reduced light transmission at this wavelength. While rotating the analyzer to a negative angle led to an overall rise in transmittance, rotating the analyzer to a positive angle decreased the transmittance peak at 480 nm, thus causing a color contrast between the positive and negative angles. Similar results were also found for Fe_3O_4@PANI-ES chiral structures (**Fig. 3c**). At 0°, the spectra showed a dominant transmittance at 480 nm and a broadband transmittance from 500 nm to 700 nm due to the relatively weak absorption in this spectral range. While decreasing the analyzer angle led to an overall increase in transmittance, with light being transmitted primarily from 480 nm to 600 nm, increasing the analyzer angle resulted in a drop in peak at shorter wavelengths (< 600 nm) and a rise in peak at longer wavelengths (> 600 nm). The overall increased transmittance for both samples relates to the analyzer angle approaching the polarization rotation from the optical activity of the chiral superstructures, allowing more light to pass through. The above results showed that both Fe_3O_4@PANI-EB and Fe_3O_4@PANI-ES chiral structures transmitted blue light near 480 nm under ORD measurements and could selectively transmit red light near 700 nm and green light near 550 nm, respectively. The pH-responsive ORD properties of Fe_3O_4@PANI may be utilized for applications in optical switches and information encryption, as demonstrated below.

Applications in Optical Switch and Information Encryption. An ORD-based optical switch was designed by exploiting the rich pH-responsive color variances, as illustrated in **Fig. 4a**. Under light illumination produced using a flower-patterned photomask, the assembled chiral structures between crossed polarizers exhibited purple and cyan colors under basic and acidic conditions, respectively. Upon rotating the analyzer, the flower pattern switched to other distinct colors, as shown in **Fig. 4b**. In this case, the colors could be dynamically modulated

by varying the analyzer angles, pH of the dispersion, and the external magnetic field (Supporting Video 1, 2).

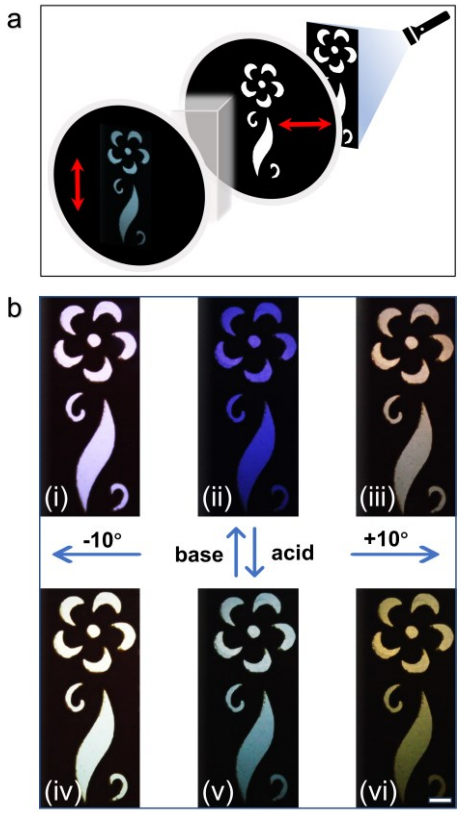

Figure 4. ORD-based optical switch under patterned light. (a) Schematic illustration of creating color patterns under polarizers. A photomask was used to generate the patterned light. The magnet with different orientations was applied but omitted in the scheme. The red arrows indicate the polarization direction of the polarizers. (b) Digital images of flower-shaped patterned light passing through aqueous dispersion of assembled Fe_3O_4@PANI superstructures with (i-iii) EB and (iv-vi) ES form under different analyzer angles at -10°, 0°, and +10°. All digital images share the same scale bar of 2 mm.

We have further explored embedding the chiral superstructures into hydrogel films for more versatile applications. To this end, we prepared Fe_3O_4@PANI/polymer composite films with chiral alignment by UV-curing aqueous mixtures of Fe_3O_4@PANI nanorods and a polyacrylamide pre-gel under a gradient magnetic field.[37] The chiral alignment of hybrid

nanorods in the gel was confirmed by the CD measurement (**Fig. 5a**). The hybrid film exhibited characteristic CD signals in both base and salt forms and showed transmitted color changes under the ORD measurement, similar to that of the colloidal dispersions (Fig. S5).

The transmittance spectra of the films were measured, as shown in **Fig. 5b**. The spectra revealed that the Fe_3O_4@PANI-EB film tended to transmit red lights (600 nm to 700 nm), whereas the Fe_3O_4@PANI-ES film inclined to transmit green lights (500 to 550 nm). Therefore, when we changed the light source to monochromic light using the light-emitting diodes (LEDs), more contrasting colors were created between the base and salt forms (Fig. S6). For instance, when using a 660-nm LED light during the ORD measurement, only the Fe_3O_4@PANI-EB film exhibited red color, while the Fe_3O_4@PANI-ES film was black since all the red light was blocked. In contrast, if a 530-nm LED light was used, the Fe_3O_4@PANI-ES film would turn green, while the Fe_3O_4@PANI-EB film became black.

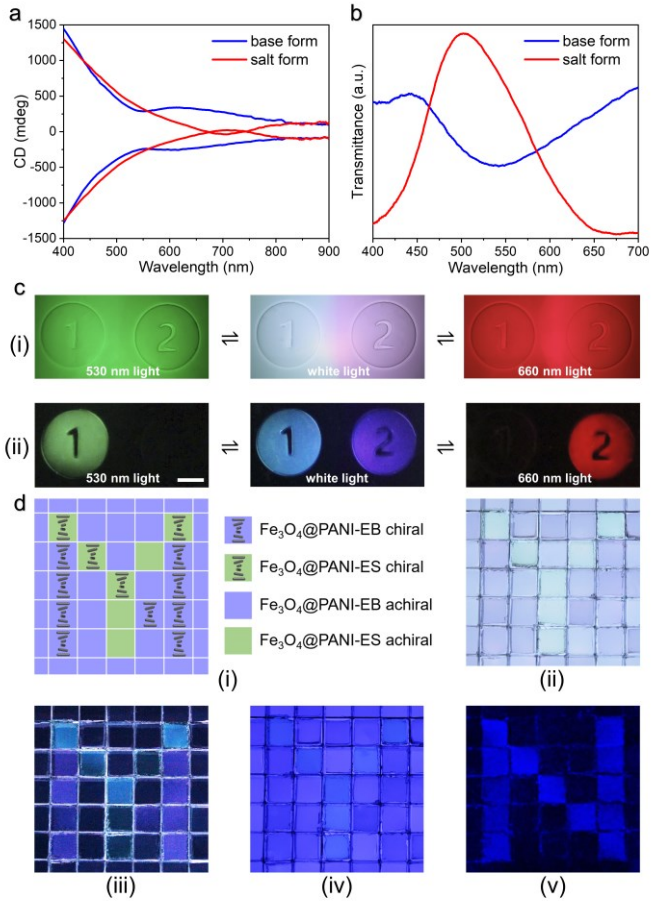

Figure 5. Chiral Fe_3O_4@PANI gels for information encryption applications. (a) CD and (b) transmittance spectra under crossed polarizers of the composite hydrogel, showing the preservation of the chiroptical properties of chiral Fe_3O_4@PANI. (c) ORD-based encryption pattern under (i) normal light and (ii) crossed polarizers. The left half of the film containing the number "1" was doped with protons, while the right half containing the number "2" was undoped. All digital images share the same scale bar of 5 mm. (d) Information encryption system selectively showing "Y" and "N" letters under different lighting conditions: (i) schematic illustration, (ii) under unpolarized white light, (iii) under white light and crossed polarizers, (iv) under unpolarized 460-nm, and (v) under 460-nm light and crossed polarizers. The dimension of each grid is 5 mm × 5 mm.

The responsive ORD property was employed for constructing an information encryption pattern to showcase the potential applications. As shown in **Fig. 5c**, the Fe_3O_4@PANI gel was fabricated to display the digital numbers "1" and "2". The chiral structures were formed within the circle, except for the numeral regions. The left half of the film containing the number "1" was doped with protons, while the right half containing the number "2" was undoped. Under unpolarized white light, the left and right sides of the film appeared cyan and lavender, respectively. Under monochromic light, the two sides showed the same color with different brightness due to the difference in transmission. However, a significant color contrast was observed when the film was under crossed polarizers. In this case, the background was black since the particles were achiral; thus, all the incoming light was blocked. Under white light, the left circle in the film appeared blue, while the right circle was purple. When the light source was changed to a 530-nm LED, the number "2" disappeared, leaving only the green circle containing the number "1". On the other hand, when a 660-nm LED was used, the number "1" would disappear, showing the red circle with the number "2". Therefore, with this design, various patterns could be selectively switched on and off by changing the wavelength of light. The film had various color changes under different lighting conditions (*i.e.*, wavelength and polarization state), promising for anti-counterfeiting applications with multi-pattern displays. Additionally, the hybrid film can be stored in ethylene glycol for over 15 months without compromising the chiral superstructures or chiroptical properties, as evidenced by the preserved ORD colors shown in Figure S7.

The potential application for information encryption was further demonstrated using a composite film comprising four different films (salt form or base form; chiral aligned or unaligned). Under the illumination of unpolarized light, the color of the composite film was contingent solely upon whether it was the salt or base forms. This feature allowed us to visualize a plaintext message, determined by the color contrast between the salt and base forms.

Under cross-polarized light, only the films exhibiting chiral alignment showed color, while those without chiral alignment turned black. This shift in visual representation effectively altered the initially perceived pattern and unveiled a ciphertext message. As shown in the example in **Fig. 5d**, a letter "Y" was fabricated with predesigned arrangements of pixels inside a square array grid (Fig. 5d(i)). Under unpolarized white light, all the blocks showed colors, light green for the salt form and light purple for the base form. Therefore, we could observe the letter "Y" in green on a purple background (Fig. 5d(ii)). By switching to polarized white light, only the chiral aligned films showed color, while the unaligned films turned black, therefore the letter “Y” became the letter “N”, as shown in Fig. 5d(iii). Under unpolarized 460-nm light, however, the letter became indistinguishable from the blue background (Fig. 5d(iv)). Finally, applying 460-nm light and crossed polarizers led to the appearance of a letter "N" corresponding to blocks containing chiral assemblies, in contrast to the black background of achiral blocks (Fig. 5d(v)). Thus, the letter "N" is concealed under the letter "Y" and can only be revealed using special method (*i.e.*, with cross polarizers). In the encrypted state (*i.e.*, without crossed polarizers), no information related to the ciphertext shows, while in the decrypted state (*i.e.*, with the crossed polarizers), the interpretation of the ciphertext is not affected by the interfering text from the encrypted state. In principle, any text or picture information can be encrypted through the arrangement and combination of different blocks, and therefore, this method may be extended for designing more complex patterns for information encryption.

CONCLUSION

We have demonstrated the creation of dual-responsive chiral superstructures by assembling Fe_3O_4@PANI hybrid nanorods in a gradient magnetic field. The field chirality is adopted by the dispersed hybrid nanorods during their magnetic assembly, enabling a dual chiroptical

response toward the changes in the field direction and solution pH. The handedness of the superstructures can be dynamically tuned by switching the field direction, manifesting an inversion of the CD signal. Changing the solution pH shifts the CD peak position from 570 nm to 830 nm, allowing the transmission of linearly polarized light of selective wavelengths and producing a significant ORD effect. The dual response makes it possible to generate color patterns with varying appearance under different illumination conditions (*i.e.*, wavelength and polarization states). The potential application of the responsive chiral assemblies has been further demonstrated by constructing a reconfigurable information encryption system that could display different patterns under polarized or unpolarized light. This work showcases the potential for creating stimuli-responsive chiroptical materials by integrating responsive mechanisms into the magnetic chiral assembly approach.

METHODS

Chemicals. Iron chloride hexahydrate ($FeCl_3 \cdot 6H_2O$), polyacrylic acid (PAA, Mw=1,800), sodium dodecyl sulfate (SDS), aniline, ammonium persulfate (APS), sodium hydroxide, and 2-hydroxy-2-methylpropiophoenone were from Sigma-Aldrich. Ammonium hydroxide ($NH_3 \cdot H_2O$, 28 wt % in water) and hydrochloric acid were purchased from Fisher Scientific. Diethylene glycol (DEG) and ethylene glycol (EG) were purchased from Acros Organics. Acrylamide and N,N'-methylenebisacrylamide were purchased from Fluka. Ethanol (200 proof) was purchased from Deco Laboratories Inc. All chemicals were used directly without further purification.

Synthesis of FeOOH Nanorods. The synthesis of FeOOH nanorods followed a reported method.[29, 30] Typically, 10.812 g $FeCl_3 \cdot 6H_2O$ was dissolved in 400 mL of water. The solution

was placed in an oven at 87 °C for 18 h. The obtained FeOOH nanorods were washed three times and redispersed in 40 mL of water.

Synthesis of Fe_3O_4 Nanorods. The surface of FeOOH nanorods was modified by PAA before reduction. Typically, 2 g of PAA was dissolved in 25 mL of H_2O, followed by adding 1 mL of $NH_3 \cdot H_2O$. After stirring for 5 min, 5 mL of FeOOH solution was added, and the solution was heated at 60 °C for 24 h. The particles were washed three times and redispersed in 1 mL of water. The high-temperature polyol reduction was used to convert FeOOH into Fe_3O_4.[29] In a typical process, 14 mL of DEG was heated to 220 °C, followed by adding 200 μL of FeOOH-PAA solution. The solution was stirred at 220 °C for 7 h. After reduction, Fe_3O_4 nanorods were washed with ethanol and water and redispersed in 20 mL of water.

Synthesis of Fe_3O_4@PANI. The coating of PANI on Fe_3O_4 was adapted from a reported procedure. [31] In a typical process, 1 mL of the above Fe_3O_4 solution was added to 25 mL of H_2O, followed by the addition of 250 μL of SDS (100 mg/mL), 2.3 μL of aniline, 250 μL of APS (0.1 M) and 125 μL of HCl (1 M). The mixture was sonicated for 5 min and aged at 10 °C for 24 h. The obtained Fe_3O_4@PANI core-shell structures were then centrifuged and washed with SDS (1 mg/mL) twice and redispersed in 10 mL of SDS (1 mg/mL). HCl or NaOH was used to dope or undope the PANI shell.

Preparation of Polyacrylamide (PAM) Hydrogel Films. The hydrogel films were prepared by photopolymerization.[37] To prepare the curing solution, the core-shell nanorods were dispersed in the precursor solution of PAM, containing ethylene glycol (2 g) as the solvent, acrylamide (1 g) as the precursor, N,N'-methylenebisacrylamide (29 mg) as the cross-linker, and 2-hydroxy-2-methylpropiophoenone (6 μL) as the photoinitiator. The curing solution was transferred to the template and cured under the illumination of a 254-nm UV light for 10 min. During curing, different magnetic fields with predesigned directions were applied. The composite films with encryption patterns were prepared through a sequential curing process

using a photomask to control chiral patterning. First, a photomask matching the desired achiral regions was placed on the substrate. The sample was cured under UV exposure without the magnetic field, fixing the achiral pattern. The photomask was then removed, and a gradient magnetic field was applied across the sample. A second UV curing step was performed to lock the chiral alignment of the nanorods in the remaining exposed areas.

Characterization. Transmission electron microscope (TEM) images were taken on a Talos 120C transmission electron microscope operating at 120 kV. The extinction spectra were measured by the Ocean Optics HR2000 CG-UV-NIR high-resolution spectrometer. CD spectra were recorded using a Jasco J-815 CD spectrophotometer.

ASSOCIATED CONTENT

Supporting Information.

The following files are available free of charge.

Figures S1−S6, with additional experimental results (PDF)

Movie S1: Flower-patterned optical switch under a laterally moving magnetic field (AVI)

Movie S2: Flower-patterned optical switch under a rotating magnetic field (AVI)

AUTHOR INFORMATION

Corresponding Author

Yadong Yin − Department of Chemistry, University of California, Riverside, California 92521, United States

Email: yadong.yin@ucr.edu

Authors

Zuyang Ye − Department of Chemistry, University of California, Riverside, California 92521, United States

Zhiwei Li − Department of Chemistry, University of California, Riverside, California 92521, United States

Ji Feng − Department of Chemistry, University of California, Riverside, California 92521, United States

Chaolumen Wu − Department of Chemistry, University of California, Riverside, California 92521, United States

Qingsong Fan − Department of Chemistry, University of California, Riverside, California 92521, United States

Chen Chen − Department of Chemistry, University of California, Riverside, California 92521, United States

Jinxing Chen − Department of Chemistry, University of California, Riverside, California 92521, United States; Institute of Functional Nano and Soft Materials (FUNSOM), Jiangsu Key Laboratory for Carbon-Based Functional Materials and Devices, Soochow University, Suzhou 215123, P. R. China

Author Contributions

The manuscript was written through contributions of all authors. All authors have given approval to the final version of the manuscript.

Notes

The authors declare no competing financial interest.

ACKNOWLEDGMENTS

The authors are grateful for the financial support from the U.S. National Science Foundation (CHE-2203972). Yin also thanks the UCR Academic Senate for providing the seed funding through the Committee on Research (CoR) Grant.

REFERENCES

(1) Glavin, D. P.; Burton, A. S.; Elsila, J. E.; Aponte, J. C.; Dworkin, J. P. The Search for Chiral Asymmetry as a Potential Biosignature in our Solar System. *Chem. Rev.* **2020**, *120*, 4660-4689.

(2) Mun, J.; Kim, M.; Yang, Y.; Badloe, T.; Ni, J.; Chen, Y.; Qiu, C. W.; Rho, J. Electromagnetic chirality: from fundamentals to nontraditional chiroptical phenomena. *Light Sci. Appl.* **2020**, *9*, 139.

(3) Sallembien, Q.; Bouteiller, L.; Crassous, J.; Raynal, M. Possible chemical and physical scenarios towards biological homochirality. *Chem. Soc. Rev.* **2022**, *51*, 3436-3476.

(4) Jiang, S.; Kotov, N. A. Circular Polarized Light Emission in Chiral Inorganic Nanomaterials. *Adv. Mater.* **2022**, e2108431.

(5) Vila-Liarte, D.; Kotov, N. A.; Liz-Marzan, L. M. Template-assisted self-assembly of achiral plasmonic nanoparticles into chiral structures. *Chem. Sci.* **2022**, *13*, 595-610.

(6) Lv, J.; Gao, X.; Han, B.; Zhu, Y.; Hou, K.; Tang, Z. Self-assembled inorganic chiral superstructures. *Nat. Rev. Chem.* **2022**, *6*, 125-145.

(7) Lee, H. E.; Ahn, H. Y.; Mun, J.; Lee, Y. Y.; Kim, M.; Cho, N. H.; Chang, K.; Kim, W. S.; Rho, J.; Nam, K. T. Amino-acid- and peptide-directed synthesis of chiral plasmonic gold nanoparticles. *Nature* **2018**, *556*, 360-365.

(8) Xu, L.; Wang, X.; Wang, W.; Sun, M.; Choi, W. J.; Kim, J. Y.; Hao, C.; Li, S.; Qu, A.; Lu, M.; Wu, X.; Colombari, F. M.; Gomes, W. R.; Blanco, A. L.; de Moura, A. F.; Guo, X.; Kuang, H.; Kotov, N. A.; Xu, C. Enantiomer-dependent immunological response to chiral nanoparticles. *Nature* **2022**, *601*, 366-373.

(9) Gonzalez-Rubio, G.; Mosquera, J.; Kumar, V.; Pedrazo-Tardajos, A.; Llombart, P.; Solis, D. M.; Lobato, I.; Noya, E. G.; Guerrero-Martinez, A.; Taboada, J. M.; Obelleiro, F.; MacDowell, L. G.; Bals, S.; Liz-Marzan, L. M. Micelle-directed chiral seeded growth on anisotropic gold nanocrystals. *Science* **2020**, *368*, 1472-1477.

(10) Kuzyk, A.; Schreiber, R.; Fan, Z.; Pardatscher, G.; Roller, E. M.; Hogele, A.; Simmel, F. C.; Govorov, A. O.; Liedl, T. DNA-based self-assembly of chiral plasmonic nanostructures with tailored optical response. *Nature* **2012**, *483*, 311-314.

(11) Probst, P. T.; Mayer, M.; Gupta, V.; Steiner, A. M.; Zhou, Z.; Auernhammer, G. K.; Konig, T. A. F.; Fery, A. Mechano-tunable chiral metasurfaces via colloidal assembly. *Nat. Mater.* **2021**, *20*, 1024-1028.

(12) Kang, L.; Lan, S.; Cui, Y.; Rodrigues, S. P.; Liu, Y.; Werner, D. H.; Cai, W. An Active Metamaterial Platform for Chiral Responsive Optoelectronics. *Adv. Mater.* **2015**, *27*, 4377-4383.

(13) Wang, Z.; Jing, L.; Yao, K.; Yang, Y.; Zheng, B.; Soukoulis, C. M.; Chen, H.; Liu, Y. Origami-Based Reconfigurable Metamaterials for Tunable Chirality. *Adv. Mater.* **2017**, *29*, 1700412.

(14) Lan, X.; Wang, Q. Self-Assembly of Chiral Plasmonic Nanostructures. *Adv. Mater.* **2016**, *28*, 10499-10507.

(15) Kuzyk, A.; Schreiber, R.; Zhang, H.; Govorov, A. O.; Liedl, T.; Liu, N. Reconfigurable 3D plasmonic metamolecules. *Nat. Mater.* **2014**, *13*, 862-866.

(16) Liu, N.; Liedl, T. DNA-Assembled Advanced Plasmonic Architectures. *Chem. Rev.* **2018**, *118*, 3032-3053.

(17) Lv, J.; Ding, D.; Yang, X.; Hou, K.; Miao, X.; Wang, D.; Kou, B.; Huang, L.; Tang, Z. Biomimetic Chiral Photonic Crystals. *Angew. Chem. Int. Ed.* **2019**, *58*, 7783-7787.

(18) Nguyen, H. Q.; Hwang, D.; Park, S.; Nguyen, M. T.; Kang, S. S.; Tran, V. T.; Lee, J. One-Pot Synthesis of Magnetoplasmonic Au@Fe_xO_y Nanowires: Bioinspired Bouligand Chiral Stack. *ACS Nano* **2022**, *16*, 5795-5806.

(19) Qi, F.; Li, L.; Li, Z.; Qiu, L.; Meng, Z.; Yin, Y. Magnetic/Plasmonic Hybrid Nanodisks with Dynamically Tunable Mechano-Chiroptical Responses. *ACS Nano* **2023**, *17*, 1427-1436.

(20) Fan, Q.; Li, Z.; Wu, C.; Yin, Y. Magnetically Induced Anisotropic Interaction in Colloidal Assembly. *Precis. Chem.* **2023**, *1*, 272-298.

(21) Jeong, K. J.; Lee, D. K.; Tran, V. T.; Wang, C.; Lv, J.; Park, J.; Tang, Z.; Lee, J. Helical Magnetic Field-Induced Real-Time Plasmonic Chirality Modulation. *ACS Nano* **2020**, *14*, 7152-7160.

(22) Li, Z.; Fan, Q.; Ye, Z.; Wu, C.; Wang, Z.; Yin, Y. A magnetic assembly approach to chiral superstructures. *Science* **2023**, *380*, 1384-1390.

(23) Chen, X.; Ye, Z.; Yang, F.; Feng, J.; Li, Z.; Huang, C.; Ke, Q.; Yin, Y. Magnetic cellulose microcrystals with tunable magneto-optical responses. *Appl. Mater. Today* **2020**, *20*, 100749.

(24) Li, Z.; Yang, F.; Yin, Y. Smart Materials by Nanoscale Magnetic Assembly. *Adv. Funct. Mater.* **2019**, *30*, 1903467.

(25) Zhang, L.; Wang, H. X.; Li, S.; Liu, M. Supramolecular chiroptical switches. *Chem. Soc. Rev.* **2020**, *49*, 9095-9120.

(26) Liu, S.; Liu, X.; Yuan, J.; Bao, J. Multidimensional Information Encryption and Storage: When the Input Is Light. *Research* **2021**, *2021*, 7897849.

(27) Jiang, N.; Shao, L.; Wang, J. (Gold nanorod core)/(polyaniline shell) plasmonic switches with large plasmon shifts and modulation depths. *Adv. Mater.* **2014**, *26*, 3282-3289.

(28) Kaissner, R.; Li, J.; Lu, W.; Li, X.; Neubrech, F.; Wang, J.; Liu, N. Electrochemically controlled metasurfaces with high-contrast switching at visible frequencies. *Sci. Adv.* **2021**, *7*, eabd9450.

(29) Xu, W.; Wang, M.; Li, Z.; Wang, X.; Wang, Y.; Xing, M.; Yin, Y. Chemical Transformation of Colloidal Nanostructures with Morphological Preservation by Surface-Protection with Capping Ligands. *Nano Lett.* **2017**, *17*, 2713-2718.

(30) Li, B.; Chen, J.; Han, L.; Bai, Y.; Fan, Q.; Wu, C.; Wang, X.; Lee, M.; Xin, H. L.; Han, Z.; Yin, Y. Ligand-Assisted Solid-State Transformation of Nanoparticles. *Chem. Mater.* **2020**, *32*, 3271-3277.

(31) Xing, S.; Tan, L. H.; Yang, M.; Pan, M.; Lv, Y.; Tang, Q.; Yang, Y.; Chen, H. Highly controlled core/shell structures: tunable conductive polymer shells on gold nanoparticles and nanochains. *J. Mater. Chem.* **2009**, *19*, 3286.

(32) Bartonek, M.; Sariciftci, N. S.; Kuzmany, H. Resonance Raman spectroscopy of the emeraldine insulator-to-metal phase transition. *Synth. Met.* **1990**, *36*, 83-93.

(33) Florea, L.; Fay, C.; Lahiff, E.; Phelan, T.; O'Connor, N. E.; Corcoran, B.; Diamond, D.; Benito-Lopez, F. Dynamic pH mapping in microfluidic devices by integrating adaptive coatings based on polyaniline with colorimetric imaging techniques. *Lab Chip* **2013**, *13*, 1079-1085.

(34) Yang, Y.; Zhang, J.; Zou, W.; Wu, S.; Wu, F.; Xie, A.; Wei, Z. Self-Assembled 3D Helical Hollow Superstructures with Enhanced Microwave Absorption Properties. *Macromol. Rapid Commun.* **2018**, *39*, 1700591.

(35) Yang, Y.; Liang, J.; Pan, F.; Wang, Z.; Zhang, J.; Amin, K.; Fang, J.; Zou, W.; Chen, Y.; Shi, X.; Wei, Z. Macroscopic helical chirality and self-motion of hierarchical self-assemblies induced by enantiomeric small molecules. *Nat. Commun.* **2018**, *9*, 3808.

(36) Kane-Maguire, L. A.; Wallace, G. G. Chiral conducting polymers. *Chem. Soc. Rev.* **2010**, *39*, 2545-2576.

(37) Li, Z.; Jin, J.; Yang, F.; Song, N.; Yin, Y. Coupling magnetic and plasmonic anisotropy in hybrid nanorods for mechanochromic responses. *Nat. Commun.* **2020**, *11*, 2883.

For Table of Contents Only: